

X-ray Absorption Line Diagnostics of Quasar Outflows

G. Chartas

Department of Astronomy & Astrophysics, Penn State University, University Park, PA 16802

Abstract. *XMM-Newton* and *Chandra* observations of quasars suggest the presence of high-velocity outflows of ionized absorbing material with mass-outflow rates of up to a few $M_{\odot} \text{ yr}^{-1}$ that are considerably higher than those based on the wind properties derived from UV BALs. Quasar winds might be more powerful than what we previously thought. X-ray absorption lines produced by outflowing material detected in several quasars is possibly probing a highly ionized and high velocity component of the accretion disk wind that appears to be distinct from the absorbers detected in the optical and UV wavebands. We present X-ray absorption line diagnostics that allow us to constraint the properties of the outflowing wind in quasars.

Keywords: <galaxies: active, galaxies: quasars, X-rays:general >

PACS: <PACS Category 90>

INTRODUCTION

Active Galactic Nuclei (AGNs) interact with their environments through outflowing winds, collimated jets, radiation that spans almost the entire electromagnetic spectrum and gravitation. It is now thought that AGNs, especially the most luminous quasars, may be regulating the growth of their host galaxies by heating the IGM gas and quenching star formation. Several recent discoveries that point to a possible feedback link between the central black hole, AGNs nuclear activity and the host galaxy are :

(a) the relation between the mass of the black hole and the velocity dispersion of the stars in the bulge of the host galaxy [e.g., 23, 16, 15, 25], (b) the very fast, and high velocity outflows of X-ray absorbing material from quasars (see references listed in Table 1), (c) the recent findings suggesting that the evolution of the space density of AGNs is strongly dependent on X-ray luminosity (L_X), with the peak space density of AGNs moving to higher redshifts for more luminous AGNs [18, 38], and (d) the recent evidence indicating a redshift-dependent correlation of the X-ray spectral slope of radio-quiet AGNs with X-ray luminosity [14, 32]. The evolution of the X-ray spectral shape of AGNs can be interpreted as an evolution of the accretion process in AGNs.

The fraction ϵ_k of the total bolometric energy released over a quasar's lifetime into the ISM and IGM in the form kinetic energy injection scales as v^3 , where v is the terminal velocity of the wind. Typical outflow velocities of X-ray absorbers in Seyfert galaxies range up to a few thousand km s^{-1} , whereas, recent X-ray observations of quasars imply outflow velocities of up to $0.7c$. We therefore expect that outflows in quasars offer a more efficient means of transporting kinetic energy to large scales. Estimating the mass outflow rates and efficiency of quasar outflows is critical in determining their importance in contributing to the feedback process.

The kinematic and ionization properties of nearby Seyfert 1 galaxies have been well studied [e.g., 10, 20, 33, 21, 27, 11] and we will borrow several of the absorption diagnostics used in the analysis of Seyfert X-ray spectra to constrain the properties of the more luminous and distant quasars.

We present several observational methods of constraining the properties of the outflowing winds in quasars. We apply these methods to several BAL quasars to constrain the mass outflow rates and efficiencies of their outflows. We finally suggest improvements that can be made to the X-ray spectral analysis that may lead to a better understanding of quasar winds.

Throughout this paper we adopt a Λ -dominated cosmology with $H_0 = 70 \text{ km s}^{-1} \text{ Mpc}^{-1}$, $\Omega_\Lambda = 0.7$, and $\Omega_M = 0.3$.

DIAGNOSTICS OF QUASAR OUTFLOWS

X-rays of sufficient energy can be absorbed by C to Ni ions and excite or eject inner K or L shell electrons resulting in the creation of K and L shell absorption lines or edges. The most common X-ray absorption lines are produced by the absorption of X-rays by H-like and He-like ions. When the absorbers are part of a quasar outflow the X-ray lines are blueshifted relative to the systemic velocity of the quasar.

With the launch of the *Chandra* X-ray Observatory, the *XMM-Newton* Observatory and the *Suzaku* X-ray satellite it has been possible to infer the kinematic and ionization properties of highly ionized X-ray absorbers. These X-ray telescopes combine the collecting area and energy resolution needed to resolve and detect the most significant absorption lines. Most current studies of X-ray absorption of AGNs have involved nearby Seyfert galaxies that are bright enough to be observed with X-ray gratings. In this paper we will mostly present studies of X-ray absorption in the most luminous and distant quasars. Because of the poor-to-medium S/N of the X-ray spectra of most high redshift quasars, current studies of absorption in these systems are made with bare CCDs that provide poor spectral resolution. We list several properties of outflowing absorbers that can be constrained from observed X-ray absorption lines in quasar spectra.

(1) Kinematic Properties

The energy of a blueshifted absorption line provides an estimate of the projected velocity of the outflowing absorber along the observed line of sight. One of the difficulties in estimating the absorber outflow velocity is the identification of the element and ionization level of the ion responsible for the absorption. This identification becomes even more difficult with low resolution spectroscopy. To illustrate X-ray absorption lines that can arise in a quasar we show in Figure 1 the absorption spectrum of a $z = 1.72$ quasar in the $1 - 10 \text{ \AA}$ rest-frame range as derived with the photoionization code XSTAR assuming a slab-like stationary absorber with $N_H = 9 \times 10^{22} \text{ cm}^{-2}$, $\log \xi = 2$, and $\log \xi = 3.5$. At ionization levels of $\log \xi \sim 3.5$ and rest-frame wavelengths in the range $1.5-2 \text{ \AA}$ (see panel a of Figure 1) the Fe lines are quite isolated and are therefore apparent even with low-resolution spectroscopy. At rest-frame wavelengths in the range of $6.2-10 \text{ \AA}$ and at ionization parameters of $\log \xi \sim 2$ the spectra contain a larger density of strong absorption lines that are difficult to resolve and identify (see panel b of Figure 1).

For high velocity flows a special-relativistic correction has to be applied and an angle

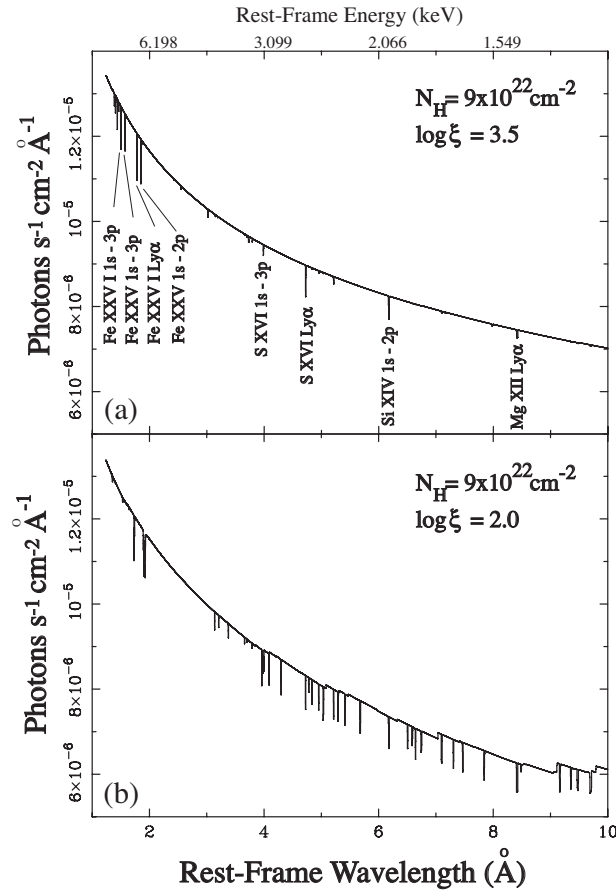


FIGURE 1. XSTAR simulations of absorbed spectra with the continuum level normalized to that of PG 1115+080. In panels a and b we show the absorbed spectra for ionization parameters of $\log \xi = 3.5$ and $\log \xi = 2.0$, respectively

between the wind velocity and our line of sight needs to be assumed. This angle is not constrained with the present data; however, hydrodynamical simulations indicate that the BAL wind divergence angle may range between 10° – 30° depending on the location of the inner radius of the disk.

For most outflows we expect the absorption line to be significantly broadened if there is a significant velocity gradient along the outflow. In this case a useful parameter that can be constrained is the maximum outflow velocity. This maximum velocity is likely produced by gas that has reached its terminal velocity. This terminal velocity is often approximated with the escape velocity from the region from which the wind is launched, resulting in the approximation $R_{\text{launch}} \sim R_s (c/v_{\text{obs}})^2$, where v_{obs} is the observed outflow velocity and R_s is the Schwarzschild radius.

(2) Ionization Parameter

It is commonly thought that the outflowing gas observed in absorption is photoionized by a central source. The degree of ionization of the absorber is characterized by the ionization parameter. Two commonly used definitions of the ionization parameter are: (a) The ionization parameter U defined as the number of ionizing photons at the ionizing

face of the absorbing gas divided by the number density of the gas (number density of H nuclei or free electron density) and is given by the expression :

$$U = \int_{\nu_0}^{\infty} \frac{L_{\nu} h \nu}{4\pi r^2 n c} d\nu \quad (1)$$

(b) The ionization parameter ξ , defined as the ionizing flux at the face of the gas divided by the number density of free electrons and is given by the expression:

$$\xi = \frac{4\pi F}{n} \quad (2)$$

The ionization parameter U for outflowing absorbers in Seyfert 1s is found to span a large range (even within an individual AGN). Specifically, the observed ranges of U for UV and X-ray absorbers are $\log(U) \sim -4$ to 0 and $\log(U) \sim -1.4$ to 1.0, respectively. Available computer programs for calculating the physical conditions and emission spectra of photoionized gases are Cloudy¹ and XSTAR².

(3) Structure of Outflows

The commonly accepted wind geometry is the unified BAL model [e.g., 40, 26, 30] In this model the AGN outflow originates in the accretion disk. This wind rises initially almost perpendicular to the accretion disk and becomes more radial and equatorial at larger radii to form a bi-cone. The unified BAL model proposes that most of the observed range of absorption line-widths can be explained with orientation and with a velocity gradient in the outflowing stream. It has also been proposed that BALs are quasars at an early stage in their evolution [e.g., 3, 39, 1, 22] It is expected that the accretion-rate may be higher during the early life of a quasar and thus one would expect to detect steeper X-ray slopes in BAL vs. non-BAL quasars if the ‘‘youth hypothesis’’ is correct. In the ‘‘youth’’ model the opening angle of the outflow is very large and only a fraction (~ 10 – 20%) of quasars have these flows.

The location of the absorbers can be inferred from the variability time-scale of the absorption features and the ionization parameter of the absorber. Based on a light-travel time argument, an observed variability time-scale of t_{var} implies that the location of the absorber is $r_{abs} \sim ct_{var}/(1+z)$. If the ionization parameter of the absorber is constrained from observations then the radial location of the absorber can be estimated as :

$$r_{abs} = \left[\frac{L(H)}{4\pi U n_e c} \right]^{0.5} \quad (3)$$

where $L(H)$ are the ionizing photons s^{-1} emitted from the central engine, and n_e is the number density of the absorber.

(4) Partial Covering

The fraction of quasars with intrinsic absorption lines can be used to infer the global covering factor. In the case where an absorber partially covers a source the profiles of the absorption lines can be used to infer the covering factor $C(\nu)$, the fraction of the

¹ <http://www.nublado.org/>

² <http://heasarc.gsfc.nasa.gov/docs/software/xstar/xstar.html>

emission intercepted by the absorber over the line of sight. This method is often applied in the case of an absorption doublet and can provide the velocity dependent covering factor and the optical depth of the absorber. Currently the covering factor method using doublets has been applied successfully to the analysis of UV spectra of AGNs, however, because of the poor S/N of available X-ray spectra of distant quasars it has not been possible to apply the doublet method to these objects in the X-ray band. For the case where there is partial covering, one expects the estimated hydrogen column density to be even larger than the value estimated assuming a neutral absorber.

The X-ray spectra of BAL quasars typically show significant residuals below 1 keV in the rest-frame band indicating the presence of possible absorption. The nature of this absorption is unclear at present, however, models that include an ionized absorber or partial covering provide better fits than models that assume a neutral absorber. A crude estimate of the covering fraction of an X-ray absorber of a BAL quasar can be obtained by fitting the X-ray spectrum with a partial covering model of the form,

$$I(E) = Ce^{-N_H\sigma(E)} + (1 - C) \quad (4)$$

where N_H is the equivalent hydrogen column of the intrinsic absorber, $\sigma(E)$ is the photoelectric cross-section and C is the covering fraction.

(5) Effective Hydrogen Column Density

The observed equivalent widths of X-ray absorption lines can be used to estimate the hydrogen column densities of the X-ray BALs by using a curve-of-growth analysis [36]. The ion species responsible for the X-ray absorption need to be known, however, this can be difficult in the case of low resolution spectra. For a crude calculation we can assume b parameters of the order of the observed widths of the lines ($b = \sqrt{2}\sigma_u$, where σ_u is the velocity width of the line).

In Figure 2 we show the curve-of-growth for the two absorption lines at 8.05 and 9.79 keV detected in the 2002 February 24 *Chandra* observation of APM 08279+5255. For no ionization correction and assuming solar abundances, the implied total hydrogen column density of these absorbers is $N_H \sim 1 \times 10^{23} \text{ cm}^{-2}$.

We emphasize that there are significant limitations with the present curve-of-growth analysis; the absorption lines may contain multiple unresolved components implying that the equivalent widths and b parameters used should be considered as upper limits. In addition, the velocity widths estimated from fits of Gaussian lines to observed absorption features can only be used to derive b parameters when the absorber is optically thin.

(6) Mass Outflow rates

Our constraints on the velocity, column density and location of the BAL material allow us to estimate the mass outflow rate from the expression:

$$\dot{M} = 4\pi r(r/\Delta r)N_H m_p v_{wind} f_c. \quad (5)$$

(7) Efficiency of Quasar Outflow

Combining the constraints on the mass-outflow rate and the bolometric luminosity one can estimate the efficiency of a quasar outflow. The efficiency of the quasar outflow is one of the key and highly uncertain parameters used in recent theoretical models that describe black-hole growth and structure formation. The efficiency is defined as the

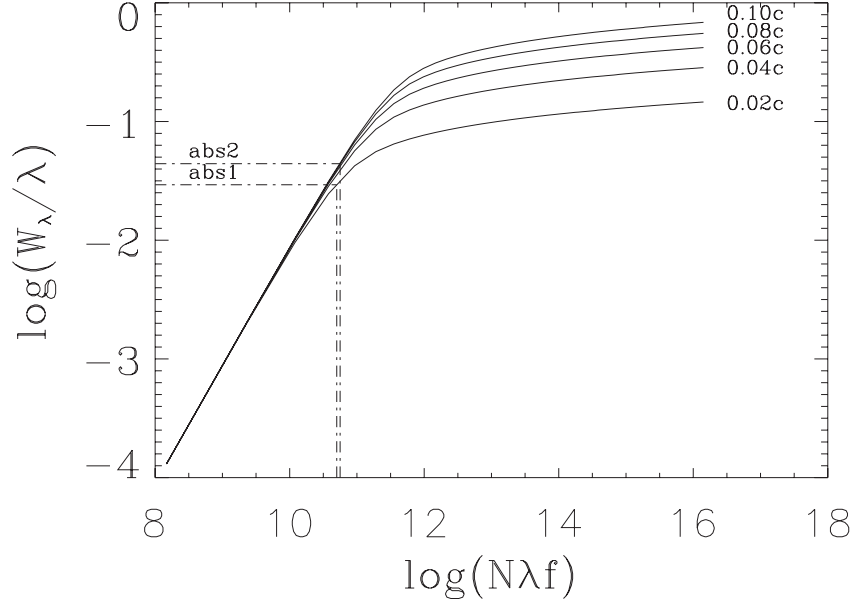


FIGURE 2. Using a curve of growth analysis one can estimate the hydrogen column densities implied by the observed equivalent widths of the two absorption lines at 8.05 and 9.79 keV detected in the 2002 *Chandra* observation of APM 08279+5255. We assumed that the ion species responsible for the X-ray BALs is Fe XXV and b parameters of the order of the observed widths of the lines.

fraction of the total bolometric energy released over a quasar's lifetime into the ISM and IGM in the form of kinetic energy injection and can be expressed as:

$$\epsilon_{k,i} = \frac{1}{2} \frac{\dot{M}_i v_{\text{wind},i}^2}{L_{\text{Bol}}} = 2\pi f_{c,i} R_i (R_i / \Delta R_i) N_{\text{H},i} m_p \frac{v_{\text{wind},i}^3}{L_{\text{Bol}}} \quad (6)$$

where \dot{M}_i is the mass-outflow rate of component i , $v_{\text{wind},i}$ is the outflow velocity of the X-ray absorber of component i , $f_{c,i}$ is the global covering fraction of the absorber of component i , ΔR_i is the thickness of the absorber at radius R_i of component i , $N_{\text{H},i}$ is the hydrogen column density of component i , and L_{Bol} is the bolometric photon luminosity of the quasar.

OBSERVED HIGH VELOCITY QUASAR OUTFLOWS

In Table 1 we list AGNs with reported detections of blueshifted absorption lines that have been interpreted as originating from fast outflows. We also note the few cases where interpretations other than AGN outflows have been provided in the literature.

We employed the absorption diagnostic techniques described in this paper to constraint the mass-outflow rates and outflow efficiencies for mini-BAL quasar PG 1115+080 and BAL quasar APM 08279+5255. We find the mass-outflow rates of PG 1115+080 and APM 08279+5255 to be about $5 M_{\odot} \text{ yr}^{-1}$. We find the outflow efficiencies of PG 1115+080 and APM 08279+5255 to be $\epsilon_k = 0.64^{+0.52}_{-0.40}$ (68% confidence), and $\epsilon_k = 0.09^{+0.07}_{-0.05}$ (68% confidence), respectively.

TABLE 1. Fast Outflows from AGNs (Table adapted from Cappi 2006)

Object	redshift	E_{rest} (keV)	$\log N_{\text{H}}$ (cm^{-2})	v_{abs} (c)	Reference
MCG-5-23-16	0.0085	6.74 and 7	22.9	0.1	[2]
IC 4329a	0.0160	7.7	22.1	0.1	[24]
IRAS 13197-1627	0.0165	7.5	23.7	0.1	[12]
Mrk 509	0.034	8.2	23.1	0.1 – 0.2	[13]
PG 0844+349	0.064	8.7	23.6	0.2	[28, 4]
PG 1211+143	0.081	7.6	22.3	0.15	[29]
PDS 456	0.184	7.6–9.3	23.7	0.16	[31]
PG 1115+080	1.72	7.3, 9.8	22.6, 23.6	0.1, 0.4	[8, 7]
H 1413+117	2.56	9, 15		0.23, 0.67	[9]
APM 08279+5255	3.91	8.1, 9.8	23, 23	0.2, 0.4	[6, 19]

These estimates include only contributions from observed components and therefore should be considered as lower limits. Our derived estimates of the efficiency of the outflows in mini-BAL quasar PG 1115+080 and BAL quasar APM 08279+5255, when compared to values predicted by recent models of structure formation [17, 34, 37], imply that these winds will have a significant impact on shaping the evolution of their host galaxies and in regulating the growth of the central black hole.

Modeling transmission and emission spectra of the ionized outflowing winds in AGNs is a complicated problem and most current analyses assume simplistic absorbers with a slab-like geometry, a uniform density, and a single bulk outflow velocity. A recent study by Schurch & Done 2007 ([35]) provides a more realistic treatment of modeling the X-ray spectra of AGNs viewed through absorbing outflowing winds by incorporating radiative transfer calculations and including velocity and density gradients. The simulated absorption features are very complex and depend strongly on the assumed velocity and density distributions, the ionization parameter and the column density. One result from Schurch & Done 2007 that differs significantly from previous studies is the sharpness of the spectra absorption features and the sensitivity of the absorption trough near the Fe $K\alpha$. In Figure 3 we show the *Chandra* spectra of mini-BAL quasar PG 1115+080 (left panel) and LoBAL quasar H 1413+117 (right panels). The notch-like absorption structures detected near the Fe $K\alpha$ line are very similar in shape to those produced in simulations that incorporate radiative transfer.

REFERENCES

1. Becker et al., 2000, ApJ, 538, 72.
2. Braito, V., et al. 2006, Astronomische Nachrichten, 327, 1067.
3. Briggs, F. H., Turnshek, D. A., & Wolfe, A. M. 1984, ApJ, 287, 549.
4. Brinkmann, W., Wang, T., Grupe, D., & Raeth, C. 2006, A&A, 450, 925
5. Cappi, M. 2006, Astronomische Nachrichten, 327, 1012.
6. Chartas, G., Brandt, W. N., Gallagher, S. C., & Garmire, G. P. 2002, ApJ, 579, 169.
7. Chartas, G., Brandt, W. N., & Gallagher, S. C. 2003, ApJ, 595, 85.
8. Chartas, G., Brandt, W. N., Gallagher, S. C., & Proga, D. 2007, AJ, 133, 1849.
9. Chartas, G., Eracleous, M., Dai, X., Agol, E., & Gallagher, S. 2007, ApJ, 661, 678.

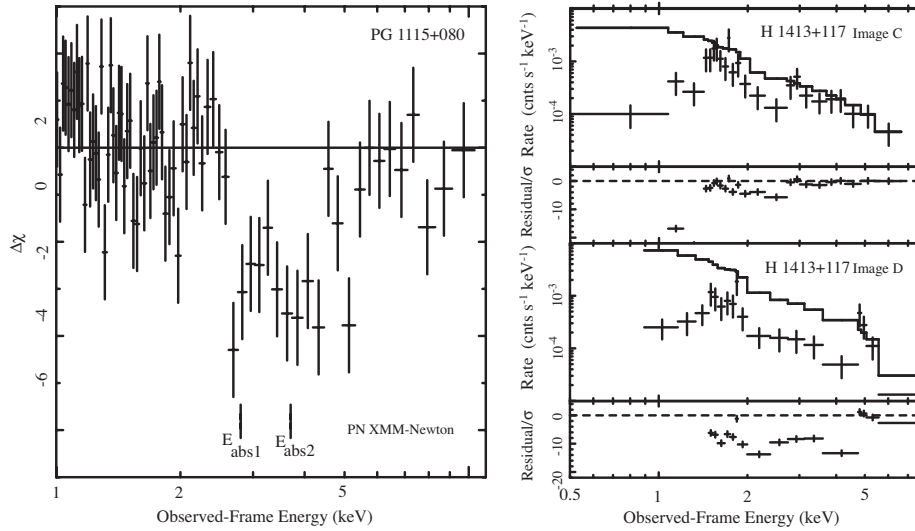


FIGURE 3. (left panel) $\Delta\chi$ residuals between the best-fit Galactic absorption and power-law model and the PN XMM-Newton spectrum PG 1115+080. (right panels) ACIS *Chandra* spectra and fit residuals of images C and D of H 1413+117.

10. Crenshaw et al. 1999, ApJ, 516, 750.
11. Crenshaw, D. M., et al. 2003, ApJ, 594, 116.
12. Dadina, M., & Cappi, M. 2004, A&A, 413, 921.
13. Dadina, M., Cappi, M., Malaguti, G., Ponti, G., & de Rosa, A. 2005, A&A, 442, 461.
14. Dai, X., Chartas, G., Eracleous, M., & Garmire, G. P. 2004, ApJ, 605, 45.
15. Ferrarese, L. & Merritt, D. 2000, ApJ, 539, L1.
16. Gebhardt et al. 2000, ApJ 539, L13.
17. Granato et al. 2004, ApJ, 600, 580.
18. Hasinger 2005, A&A, 441, 417.
19. Hasinger, G., Schartel, N., & Komossa, S. 2002, ApJL, 573, L77.
20. Kraemer, S. B., et al. 2001, ApJ, 551, 671.
21. Kaspi, S., et al. 2002, ApJ, 574, 643.
22. Lacy et al., 2002, AJ, 123, 2925.
23. Magorrian, J., et al. 1998, AJ, 115, 2285.
24. Markowitz, A., Reeves, J. N., & Braitto, V. 2006, ApJ, 646, 783.
25. McLure R. J., & Dunlop, J. S. 2002, MNRAS, 331, 795.
26. Murray, N., Chiang, J., Grossman, S. A., & Voit, G. M. 1995, ApJ, 451, 498
27. Netzer, H., et al. 2003, ApJ, 599, 933.
28. Pounds, K. A., King, A. R., Page, K. L., & O'Brien, P. T. 2003, MNRAS, 346, 1025.
29. Pounds, K. A. & Page, K. L., 2007, astro-ph/0607099.
30. Proga, D., Stone, J. M., & Kallman, T. R. 2000, ApJ, 543, 686
31. Reeves, J. N., O'Brien, P. T., & Ward, M. J. 2003, ApJL, 593, L65
32. Saez et al., F. E., Dai, X., & Garmire, G. P., 2007, submitted to ApJ.
33. Sako, M., et al. 2001, A&A, 365, L168.
34. Scannapieco, E., & Oh, S. P. 2004, ApJ, 608, 62. Scannapieco & Oh 2004
35. Schurch, N. J., & Done, C. 2007, ArXiv e-prints, 706, arXiv:0706.1885
36. Spitzer, L. 1978, New York Wiley-Interscience, 1978. 333 p.
37. Springel, V., Di Matteo, T., & Hernquist, L. 2005, ApJL, 620, L79.
38. Ueda et al. 2003, ApJ, 598, 886.
39. Voit, G. M., Weymann, R. J., & Korista, K. T. 1993, ApJ, 413, 95.
40. Weymann, R. J., Morris, S. L., Foltz, C. B., & Hewett, P. C. 1991, ApJ, 373, 23